A Multifunctional SiC DC-DC Converter Topology with Normalized Fault Detection Strategy for Electric Vehicle Applications

by

Brandon Pieniozek

A thesis submitted in partial fulfillment
of the requirements for the degree of
Master of Science in Engineering
(Energy Systems Engineering)
in the University of Michigan – Dearborn
2020

Thesis Committee:

Associate Professor Taehyung Kim, Chair
Assistant Professor Junho Hong
Assistant Professor Jaerock Kwon

Acknowledgements

To begin I'd like to acknowledge my parents, Mark and Cindy, for their love and support throughout my life. They have always made me a priority and encouraged me to put forth my best effort in whatever endeavor I pursue. My parents take great pride in my education and career achievements, so I'd like to dedicate this work to them. Next I'd like to acknowledge the guidance that Dr. Taehyung Kim has provided throughout the thesis process. From the very beginning he has been open to my ideas and provided helpful insight for this project. He has also worked around my schedule in order to accommodate my needs. Thank you to Dr. Taehyung Kim for helping me throughout the entirety of this project. I would like to express my gratitude to committee members Dr. Junho Hong and Dr. Jaerock Kwon for their insight and constructive feedback on the project. Finally, I'd like to recognize the department of ESE and ECE for accepting me into the program and allowing me to pursue my interests in energy systems as well as power electronics.

Table of Contents

List of Figures

Abstract

The automotive industry is experiencing a monumental shift in technology and propulsion strategies. More than ever before, car manufacturers and suppliers are shifting development and funding away from combustion engines in favor of electrified powertrains. One of the main obstacles contributing to customers reluctance to buy EVs is the lack of infrastructure for charging. Traditional 110/220VAC outlets equipped at residential buildings are relatively low power compared to the batteries used in EVs today. These AC chargers, classified as level 1 and level 2, will take approximately 12-24 hours to completely charge a battery, depending on battery size and state-of-charge. Additionally, because this method of charging uses alternating current, vehicles must have chargers on-board to convert the energy from AC to DC to recharge the battery because EV batteries are direct current energy sources. Millions of dollars from the government and private companies are being invested to create an adequate DC fast charging infrastructure. The advantages of DC charging are two-fold, much quicker charging times and the elimination of on-board chargers. However, there is one blatant problem with current investments into a DC charging infrastructure – technological advancement. Most electric vehicles in production have battery pack voltages between 300V and 400V and current DC fast chargers are being developed for the current technology. This will likely change rather quickly; the development of wide-bandgap devices will allow for higher voltage devices. Furthermore, the energy densities of batteries will also likely improve, allowing for higher bus voltages. Higher bus voltages will offer several advantages over current architectures – more power, smaller devices, improved efficiencies, and more.

The problem is, once higher bus voltages are achieved and popularized, the current fast charging infrastructure will be deemed obsolete. An intermediate solution needs to be developed to allow higher bus voltage vehicles to continue to utilize the current fast chargers being deployed nation-wide.

The proposed DC-DC converter is a practical design that offers multiple purposes when implemented in electric vehicles that utilize permanent magnet synchronous machines (PMSM) and bus voltages of ~800V. It consists of a bi-directional interleaved DC-DC cascaded with an isolated full bridge converter. This configuration provides a 12V source with galvanic isolation during normal propulsion. The interleaved converter can boost in reverse to allow for charging of the 800V bus with current generation DC fast chargers operating at ~400V. Finally, an inverter fault detection methodology has been realized to take advantage of the interleaved DC-DC structure. If an open switch fault is detected on any of the 3-phases driving the PMSM, the appropriate phase-leg is isolated, and a phase-leg from the interleaved DC-DC is used to maintain propulsion. This is realized by monitoring the phase currents of the AC motor and analyzing the difference in value between all three. A threshold value is implemented in C-code, not contingent on the system parameters. A difference of phase currents greater than the threshold value is a clear indication that an open switch fault has occurred. The proposed power conversion structure and the motor inverter fault detection, isolation, and compensation approaches are verified by a PSIM simulation. The simulation results successfully validate the feasibility of proposed electric powertrain structure and inverter switch fault detection and compensation methods.

Chapter 1: Introduction

Unbeknown to many people, electric vehicles have existed in the automobile industry since the late 1800s. It wasn't until the turn of the new century when their popularity diminished in favor of internal combustion engines. This was primarily due to two reasons, the advent of the assembly line by Henry Ford and the invention of the electric starter. The assembly line allowed Henry Ford to manufacture vehicles at one-third the price of electric competitors while the electric starter alleviated the hassle of starting an engine by hand cranking it. After being nearly irrelevant for almost a century, interest in electric vehicles has risen dramatically. We can deduce this is primarily due to the vast improvement in electrification technology, the increase in gas prices, and an awareness of how nonrenewable energies negatively impact the environment.

To achieve propulsion, an electric vehicle powertrain is composed of several essential components: a DC energy source, an inverter, and an electric motor. A couple other components are also needed in order to charge the energy source and convert the operating voltage to other necessary levels. These items are a constant focus for engineers and scientists to improve the technology in an effort to make electric vehicles more powerful and efficient.

The objective of this project was to develop a practical DC-DC converter that allows for multiple use cases compared with traditional EVs that have components which only serve a single function. Target applications would include next generation architectures that utilize silicon carbide (SiC) devices and 800V batteries. The proposed solution includes a bi-directional interleaved DC-DC converter that is cascaded with an isolated full bridge DC-DC converter. This configuration would provide a 12V source with galvanic isolation during normal propulsion and

still be flexible for additional functionality. The interleaved converter on the front-end reduces the 800V battery voltage to 400V. This is accomplished rather simply as the converter can be thought of as averaging the voltage between switching cycles; assuming switching cycles are equal, the average of 800V and 0V would be 400V. Reducing the bus voltage in half allows for a smaller full bridge converter design. Full bridge DC-DC converters work by utilizing the transformer present in the circuit. Transformers not only provide necessary protection by being galvanically isolated, but the ratio of turns between the primary and secondary winding will inherently increase or decrease the voltage at the output – this is how 12V is achieved from 400V. As previously mentioned, the premise of the converter topology was to allow for multiple functions, so the front-end converter can actually operate in reverse. This lets manufacturers utilize the current DC fast charging infrastructure being deployed across the country. When a 400V DC fast charger is plugged into the EV, the DC-DC will increase/boost the voltage to over 800V allowing the high voltage battery to charge. Finally, an inverter fault detection methodology has been realized to take advantage of the interleaved DC-DC structure. Electronics tend to degrade and possibly even fail over time – EV components are no different. As a preventative measure to avoid a vehicle suffering an inverter fault and becoming immobile, if an open switch fault is detected, the appropriate phase-leg containing the switch is isolated, and a phase-leg from the interleaved DC-DC is used to maintain propulsion. The proposed converter topology and fault detection method are verified by PSIM simulation. The simulation results successfully validate the feasibility of the power electronics system and switch fault detection strategy.

1.1 Electric Vehicle Powertrains

Electric vehicle powertrains are fairly simplistic when compared with a vehicle using a conventional combustion engine. The main components of an EV consist of a high voltage lithium-ion battery, a 3-phase AC motor, and a few power electronics modules. Batteries are constructed by placing several cells in series and parallel in order to obtain a desired pack voltage. Placing cells in series will increase the voltage of the pack while placing them in parallel will increase the packs energy density. Further, cell manufacturers will offer different cell topologies, two of the most popular being cylindrical and pouch. For example, Tesla battery packs make use of cylindrical cells while vehicles like the Chevy Bolt use pouch cells – each style of cell having benefits and drawbacks.

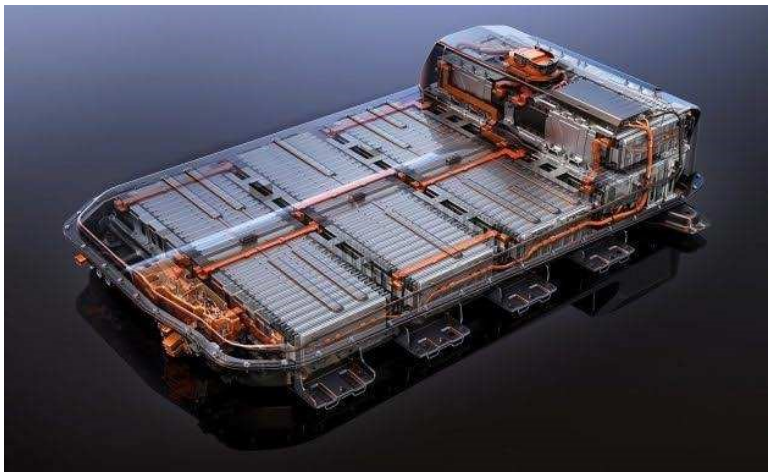

Figure 1.1: A 66kWh 350V lithium-ion battery constructed of LG pouch cells, used in the Chevrolet Bolt.

Automakers continuously work on improving battery chemistry so that they become more energy dense, and most importantly, cheaper. Advancement in energy density and the adoption of SiC devices will enable vehicles to operate with higher bus voltages. The majority of EVs today

utilize bus voltages between 300V and 400V, but future EVs will likely use 800V architectures because SiC devices have a larger breakdown voltage when compared with Si devices. A move to SiC switches will allow for higher switching frequencies, smaller passive components, higher efficiency, and more. This topic will be discussed further in a succeeding section. Next generation EV architectures, including SiC devices, were targeted for this project, so an 800V bus was used. Ultimately, the battery is perhaps the most important component in an electric vehicle as it is the vehicles primary source of energy; propulsion wouldn't be possible without it.

Electric motors are another vital component that can be found in an EV. An electric motor is a device that converts electrical energy into mechanical energy, or visa versa. These devices can be powered by DC as well as 3-phase AC. Applying a specific current through the motor will produce a given torque. There are also different styles of AC motors, including induction and synchronous. Nikola Tesla invented the first induction motor in the late 1890's in and paved the way for what is now the modern-day electrical grid. Over the past decade, synchronous machines have grown in popularity, especially in the automotive sector. The vast majority of EVs and hybrids produced today utilize a style of synchronous machine known as an interior permanent magnet (IPM) motor. They differ from induction motors in how they are constructed, but also offer several benefits. A traditional induction motor uses copper windings that are embedded into the stator and rotor. Motor operation follows laws popularized by Maxwell regarding electromagnetism. A magnetic field can be generated by an electric current or through a time-varying electric field. So, in principle, current is commanded through the stator of the motor and this current creates a rotating magnetic field. This magnetic field in the stator will then induce an electrical current in the rotor, producing torque and rotating a drive shaft. The difference between

induction motors and IPM motors is in the construction of the rotor. IPM motors, like the name suggests, use rare earth magnets instead of copper windings. The magnets are embedded inside the rotor during manufacturing.

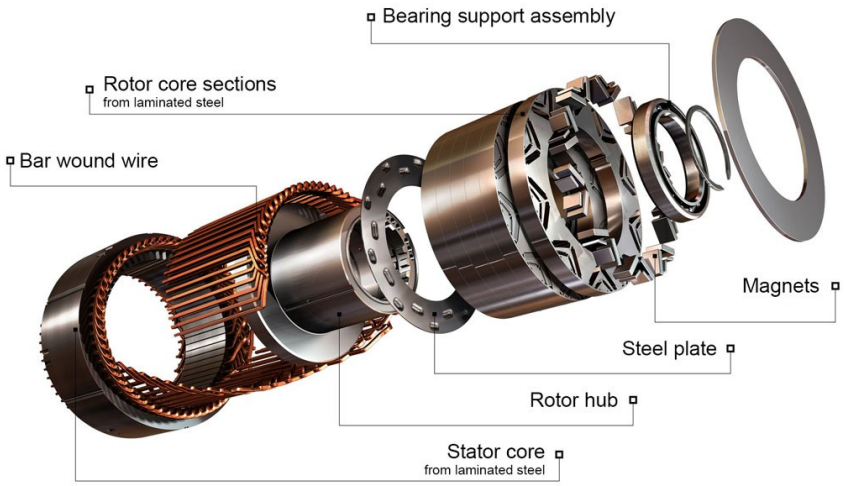

Figure 1.2: Exploded view of GM's interior permanent magnet motor used on the Chevy Bolt.

IPM motors offer several benefits compared with induction motors, including greater power density, smaller size, and being more efficient. Due to their popularity in electrical drive systems, a 3-phase permanent magnet synchronous machine (PMSM) was utilized for this project.

As stated previously, the primary items in an EV are the batteries, motor, and lastly, the power electronics. Power electronics utilize high power electronic devices to convert and control the transfer of energy. Modules will comprise of passive electronic components, solid-state switches, and drive boards. Passive components include inductors, capacitors, and resistors. With the addition of switches and proper control methodology, energy conversion can be achieved. Capacitors and inductors are passive electrical components that store energy in the form of an electrical charge or magnetic field, respectively. For an inductor, if an instantaneous voltage is

applied, the current will change over time. Likewise, with a capacitor, a current will produce a voltage that increases or decreases linearly. Equations 1 and 2 describe this behavior.

$$\text{Inductor: } V = L \times \frac{di}{dt} \tag{1}$$

$$\text{Capacitor: } I = C \times \frac{dv}{dt} \tag{2}$$

Moving onto solid-state switches, metal oxide silicon field effect transistors (MOSFETs), bipolar junction transistors (BJTs), and insulated-gate bipolar transistors (IGBTs) are the three most commonly used devices in electronics. For power electronics, Si IGBTs have been the most popular for quite some time. This is because IGBTs possess the power capabilities of BJTs while having easy control like a MOSFET. However, the demand for SiC MOSFETs has been increasingly dramatically. An electronic switch for converters is treated similar to a mechanical switch, they exist in two states, on or off. Controlling the on-time of the switch in a circuit containing an energy storage device will produce certain effects that can be used to convert voltages up or down or turn a DC/AC signal into an AC/DC signal. Such components include:

- AC-AC converters
- AC-DC rectifiers
- DC-AC inverters
- DC-DC converters

Inverter and DC-DC converters are the main focus for this project. A buck converter is perhaps the simplest DC-DC topology to understand. A traditional buck utilizes all of the passive and active components that have been discussed. This converter has a switching device in series with a voltage source, a diode, an inductor, and a capacitor.

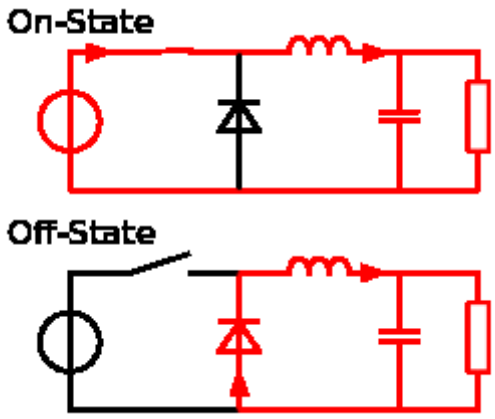

Figure 1.3: Overview of how a buck converter operates in the on and off states.

When the DC-DC is in the on-state, current passes through the switch and produces a voltage across the inductor. As a result, current will increase linearly like Eq. (1) shows. During the on-state current will charge the output capacitor and provide power to the load. During the off-state, the switch opens and the input current from the source drops to zero. The capacitor begins to discharge as it supplies power to the load and the current through the inductor decreases in the same linear fashion.

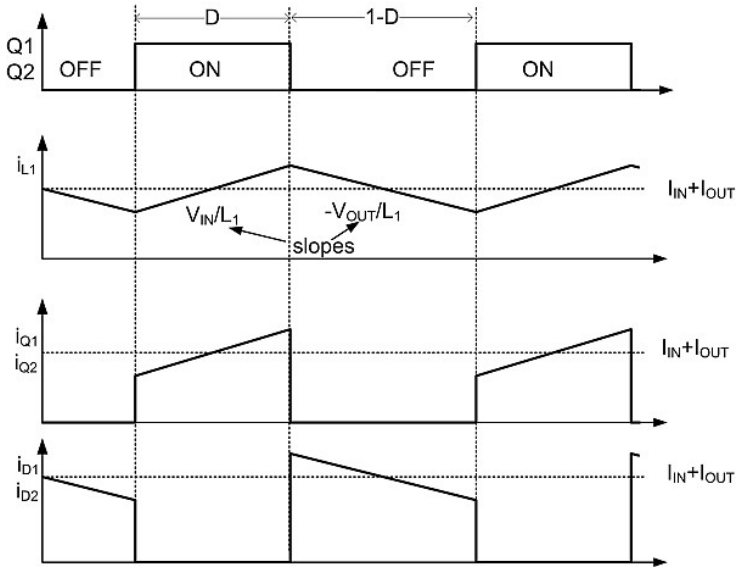

Figure 1.4: General waveforms of a buck converter.

This switching of circuit states produces a voltage at the output less than that of the input. A varying amount of 'bucked' voltage can be achieved by changing the amount of time the switch is in the on state; this is what is known as the duty cycle. The buck converter can be thought of as averaging the input voltage while having a LC filter at the output. A bi-directional and interleaved buck converter is utilized for this project. Interleaving is a term applied to converters that use multiple current paths, or phases. The converter becomes bi-directional when the passive diode is replaced with a second switch. Doing this allows the DC-DC to buck in one direction and boost in the opposite direction which will prove to be useful later. A traction inverter is similar in structure to a bi-directional interleaved converter. Three phases, each with two switches, are placed in parallel with an energy source. The load for the inverter is a 3-phase AC motor with intrinsic inductance. In particular, the motor used for this project is a PMSM. Converting power from DC to AC is as much about the control scheme as it is the hardware.

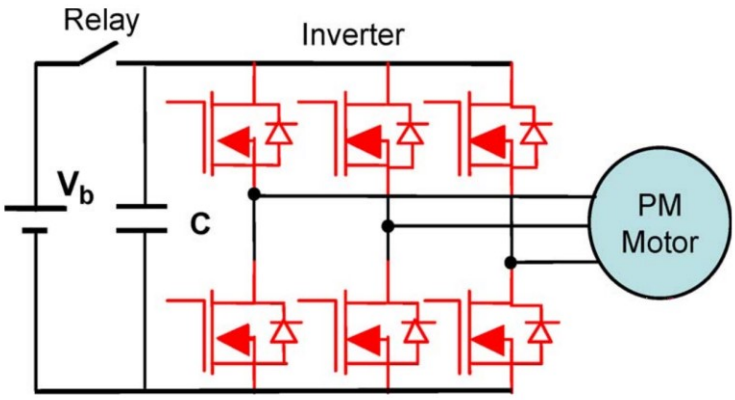

Figure 1.5: A 3-phase voltage source inverter overview with energy source and AC motor.

Advancements in semiconductor technology has improved the performance in not only discrete components, but integrated circuits and microprocessors as well. This improvement has enabled the development of more accurate and powerful control structures. One of the biggest

breakthroughs for AC drive topologies was the emergence of field-oriented control (FOC). It is also what is used in this project due to the ease of implementation and understanding on the topic. FOC works by transforming the rotating, AC phase currents, into vectors. This turns a 3-phase time and speed dependent system into a two-coordinate time invariant system [1]. The transformation grants a more simplistic control scheme similar to that of a DC motor. When used, direct torque control is realized. It also remains accurate during steady-state and transient conditions. Two transformations need to take place in order to achieve a two-variable time invariant system from a 3-variable time varying system; they are known as the Clarke and Park transformations, respectively.

$$\begin{cases} i_{s\alpha} = i_a \\ i_{s\beta} = \dfrac{1}{\sqrt{3}} i_a + \dfrac{2}{\sqrt{3}} i_b \end{cases} \tag{3}$$

$$\begin{cases} i_{sd} = i_{S\alpha} \cos\theta + i_{S\beta} \sin\theta \\ i_{sq} = -i_{S\alpha} \sin\theta + i_{S\beta} \cos\theta \end{cases} \tag{4}$$

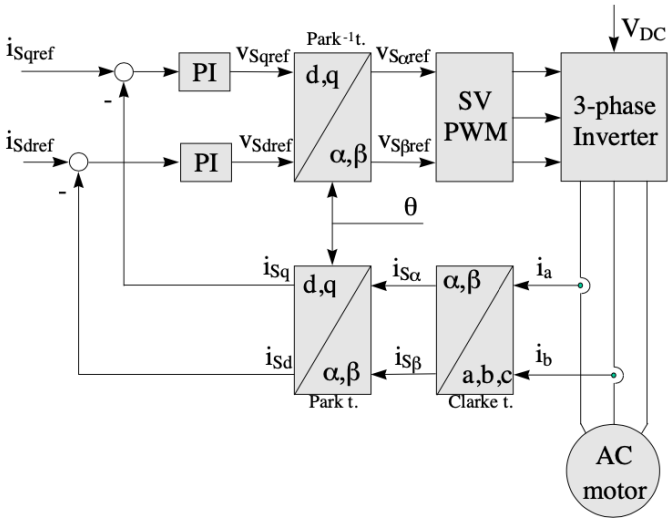

Figure 1.6: Basic interpretation of a FOC scheme.

Phase currents from the motor are measured and fed into a transform model into d and q variables. The measured results are compared with a reference and compensated with a PI controller. Finally, the signals are transformed back into the traditional 3-phase time varying variables used to control the motor torque.

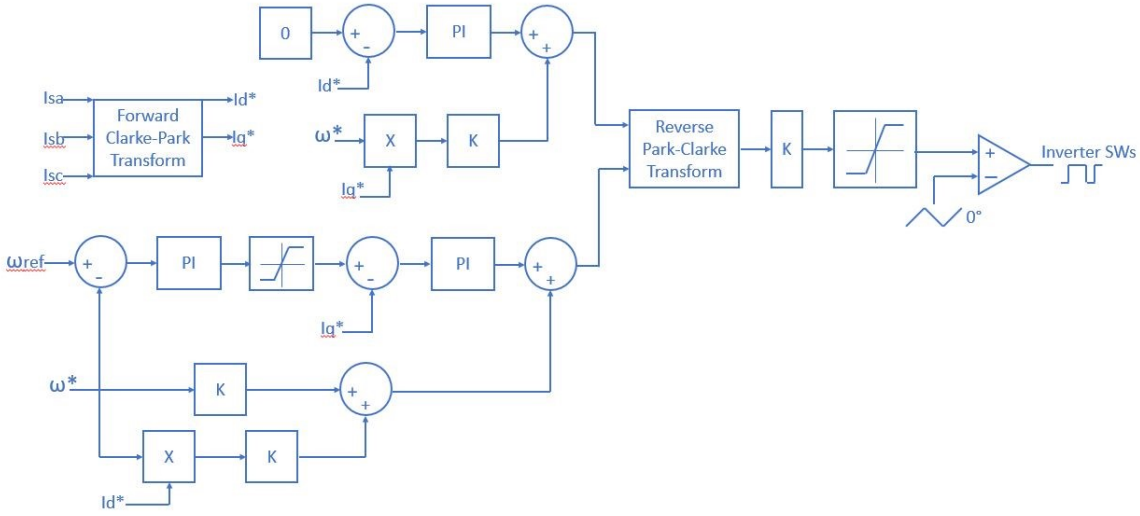

Figure 1.7: Implemented field orientated control scheme for a 3-phase PMSM in PSIM.

1.2 Next Generation Semiconductors

As previously alluded to, the key enabler for 800V vehicle architectures will be the adoption of SiC devices. SiC MOSFETs offer many performance benefits when used in electric vehicle propulsion components. They will also allow DC fast chargers to incorporate the same technology, allowing for faster, high power charging. SiC MOSFETs intrinsically possess all of the desired properties of a power switch, like a high voltage breakdown, low on-state resistance, and faster switching speeds. These characteristics combined with 800V architectures will undoubtedly render SiC MOSFETs a superior solution to Si IGBTs in traction inverters [2]. IGBT device ratings are typically between 600V-800V while most SiC power modules are rated up to 1200V; this increase in voltage is what makes 800V battery voltages possible. Headroom is required when switching semiconductor devices because fast slew rates combined with parasitic elements will lead to voltage overshoot. If the voltage exceeds the device rating, the switch will most likely fail. Higher voltages are achieved because the wide bandgap of SiC improves the ability to resist electric fields [2]. Moving on, an increase in switching frequency will improve the mass of the overall system by making certain components smaller. Considering a converter design with established requirements for input voltage, output voltage, and current ripple, if the fundamental switching frequency is increased, the value of the inductor or capacitor can be reduced, decreasing the physical size and saving space. Finally, a low on-state resistance will offer high component efficiency by minimizing power loss in the device. SiC MOSFETs not only offer great electrical properties compared with Si IGBTs, but the thermal properties are equally as impressive.

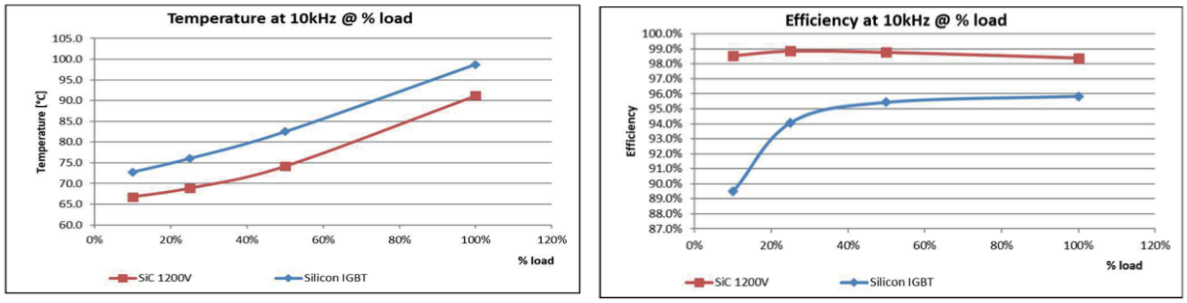

Figure 1.8: Component efficiency and thermal performance of a 1200V SiC device compared with a Si IGBT.

Performance of a Si IGBT module was evaluated against a SiC MOSFET module and the results are as expected. Considering an identical switching frequency, packaging case, and cooling structure, the thermal performance of the SiC module outperformed the Si IGBT by a factor of 3. Given the same output current, the switching frequency of the SiC module could be increased by a factor of 5. Lastly, under identical operating conditions, the power losses attributed to the switch are reduced by a factor of 4 for the SiC device [3].

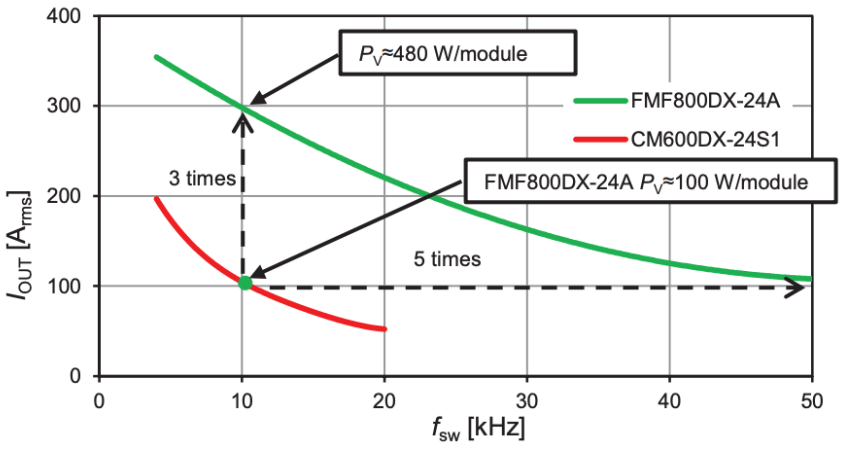

Figure 1.9: Comparison of DC and AC charging structures for an electric vehicle.

1.3 Charging Topologies and Infrastructure

Developing a fast charging infrastructure is tremendously imperative to electric vehicle adoption and silencing critics. The most common way for EVs to charge is with a traditional 110Vac or 220Vac outlet. Level 1 charging utilizes 110Vac while level 2 charging utilizes 220Vac. Electrical sockets are available nearly everywhere, but the power provided by them is extremely low making the time to charge painfully slow. For example, level 2 chargers add about 25 miles of range per hour and a level 1 charger will only provide 4 miles of range per hour [4]. To put this in perspective, a Chevy Bolt has 240 miles of range, it would take almost 10 hours to fully charge on the level 2 and about 60 hours on a level 1 charger. Even more, AC charging requires the vehicle to have an on-board charger to rectify the power and isolate the high voltage source from the low voltage source as a safety measure for the customer. In short, AC charging is slow and requires a separate component on board the EV to function.

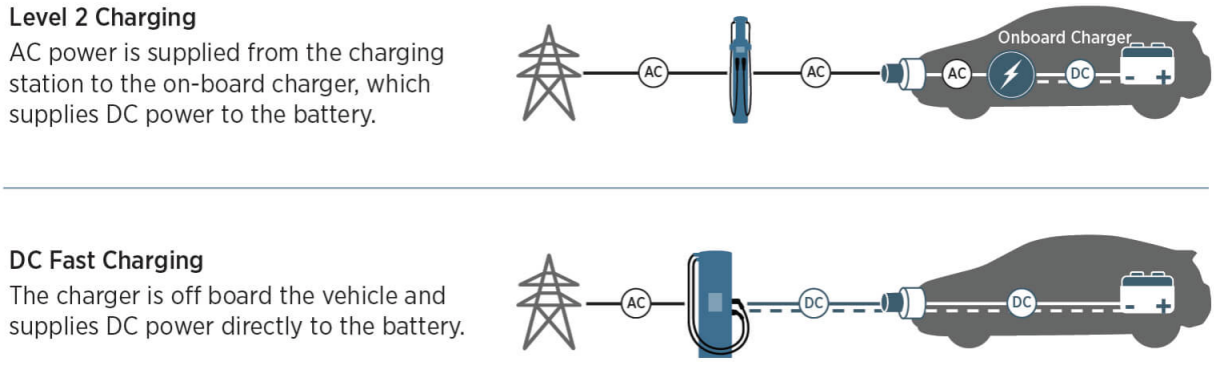

Figure 1.10: Comparison of DC and AC charging structures for an electric vehicle.

The market trend is for higher power and fasting charging times for customer convenience. Implementing DC fast charging stations is important for market penetration and mass EV adoption. These chargers need to be designed with a high-power density while remaining highly efficient

[5]. SiC technology is thus a key enabler for super-fast 800V charging technology [6]. According to SiC company Wolfspeed, benefits of SiC fast charging include 30% lower power losses, a 3x increase in switching frequency, and a 65% increase in power density over traditional methods. They also reduce component size and overall system cost by approximately 30%. Furthermore, they state that China leads the industry in charging infrastructure since they currently have about 167,000 stations with plans to deploy 4.6 million more [5]. Tesla has established one of the most extensive DC fast charger networks in the world. They have roughly 16,000 superchargers currently active, however, they only operate up to 480V. An issue will begin to manifest as current fast charging stations will be unable to charge vehicles that make use of an 800V architecture. This problem can be alleviated with investing more into developing SiC based chargers, but what will be done with the infrastructure already put in place? A simple yet effective solution for charging 800V batteries is to utilize existing components already on-board the EV to mate with current 400V DC fast chargers.

Chapter 2: Cascaded DC-DC Converter Operation

2.1 Introduction

The cascading of two DC-DC converters provides a couple essential benefits for this specific application. First, the ability to execute high voltage conversion is realized. In EVs, an isolated step-down converter is used to convert the 300-400V bus down to 12V so that normal car electronics can operate. These converters are usually a full bridge topology, but some may have an additional network of inductors and capacitors in order to form a resonant tank. Full bridge converters are great for achieving high voltage conversion due to the use of a transformer. The conversion ratio is a function of duty cycle as well as the winding ratio between the primary and secondary coils. However, converting the desired bus voltage of 800V down to 12V simply through the winding ratio is not ideal. Adding an additional converter stage allows for higher voltage conversion and for the components to be sized more appropriately. Additionally, the secondary converter was designed to be bi-directional. If optimized correctly, the bi-directional interleaved converter can serve multiple purposes.

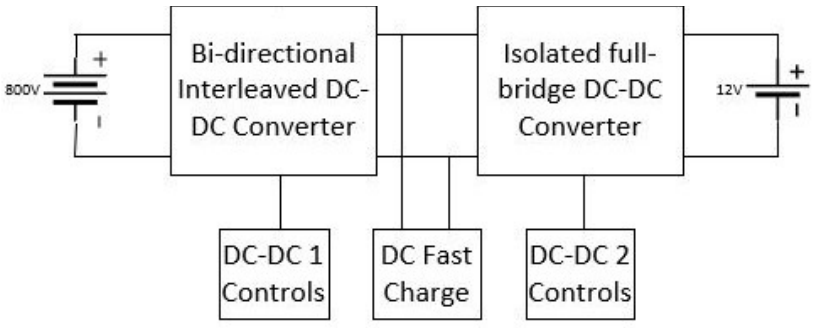

Figure 2.1: Cascaded DC-DC converter topology overview.

During propulsion the cascaded converter scheme will provide 12V to power the car electronics. In the event that an inverter switch fault is detected, a single phase of the interleaved structure can be used to replace the damaged phase in the inverter. Another application for the interleaved DC-DC is devised for DC fast charging applications. The DC fast charging infrastructure being implemented by companies around the country all currently operate with 300-400V bus architectures. Until 800V DC fast charging infrastructure is developed, cars with an 800V bus will not be able to charge using the existing chargers. This provides the opportunity to use the interleaved converters bidirectionality to boost the voltage from current DC fast chargers, to levels required to charge a vehicle with an 800V bus.

2.2 Interleaved Buck Converter

2.2.1 Overview

The interleaved buck converter was the chosen topology as the front-end converter for a couple key reasons. First, an isolated DC-DC is unnecessary for the first voltage conversion from 800V to 400V when operating during vehicle propulsion. Similarly, when operating in reverse to boost from 400V to 800V for charging the battery, an isolated DC-DC isn't required. This is in contrast to what is required for on-board chargers currently being used in modern EVs. A subsequent section will further explore this topic. Another benefit to interleaving converters is the reduction of input current ripple. Eq. (5) exhibits that the ripple current the inductor produces is a direct result of how much inductance there is. The greater the inductance value, the smaller the ripple current will be.

$$\Delta I_L = \frac{V_{OUT} \times (V_{IN} - V_{OUT})}{L \times f_S \times V_{IN}} \tag{5}$$

In addition, any inductor ripple current present in the converter will always be reflected back into the main energy source. The amount of ripple current the source can tolerate is usually a key design parameter contributing to how large the inductor is sized. By adding a secondary current leg and alternating the switching cycles by 180°, the input ripple tends to cancel due to current legs being out of phase with each other. For a 2-phase system, as the duty cycle approaches 50%, the input ripple current will be reduced to zero.

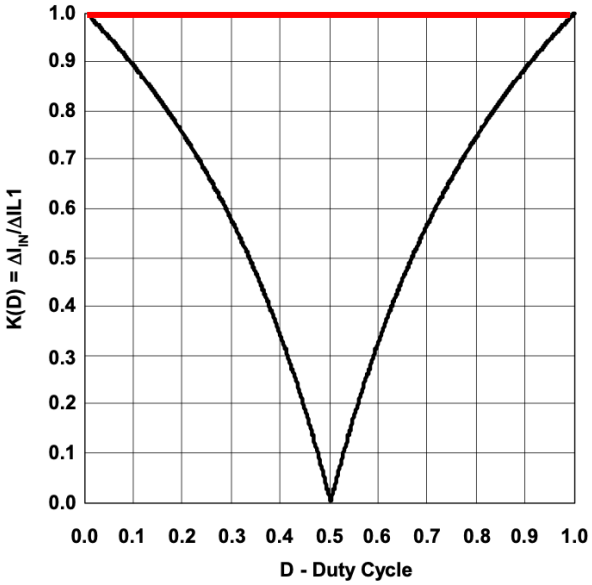

Figure 2.2: Input current ripple reduction for 2-phase converters compared with a single phase.

A simple strategy is to design the converter to operate around 0.5D in order to take advantage of the ripple cancellation properties inherent to interleaving. Likewise, interleaving will also reduce the total inductor energy by 50%, resulting in smaller inductor size [7]. This is realized because the phase legs will each take half of the total current in the system. Inductor windings are mainly constructed using copper which will possess a resistivity property. The amount of

resistance present in the winding will be intrinsic to the physical dimensions of the wire – specifically length and diameter. Like any DC component, resistance contributes to power loss.

$$P = I^2 \times R \tag{6}$$

As can be seen from Eq. (2), if the DC current through the inductor is reduced by half, the power loss due to the winding resistance will be reduced by half. A second type of power loss is also encountered due to winding eddy currents induced from a time-varying magnetic flux in the inductor core [8]. In short, interleaving phase legs will reduce the total power loss in the circuit.

The components of the converter were sized using the commonly derived buck/boost design equations while also taking into account the benefits of an interleaved topology. Moreover, the converter was designed to operate in continuous conduction mode (CCM). Operating the converter in discontinuous current mode would offer some advantages as well as some disadvantages. The circuit was built and simulated in PSIM using four SiC MOSFET switches, two inductors, and one output capacitor. All components were given some basic parasitic properties.

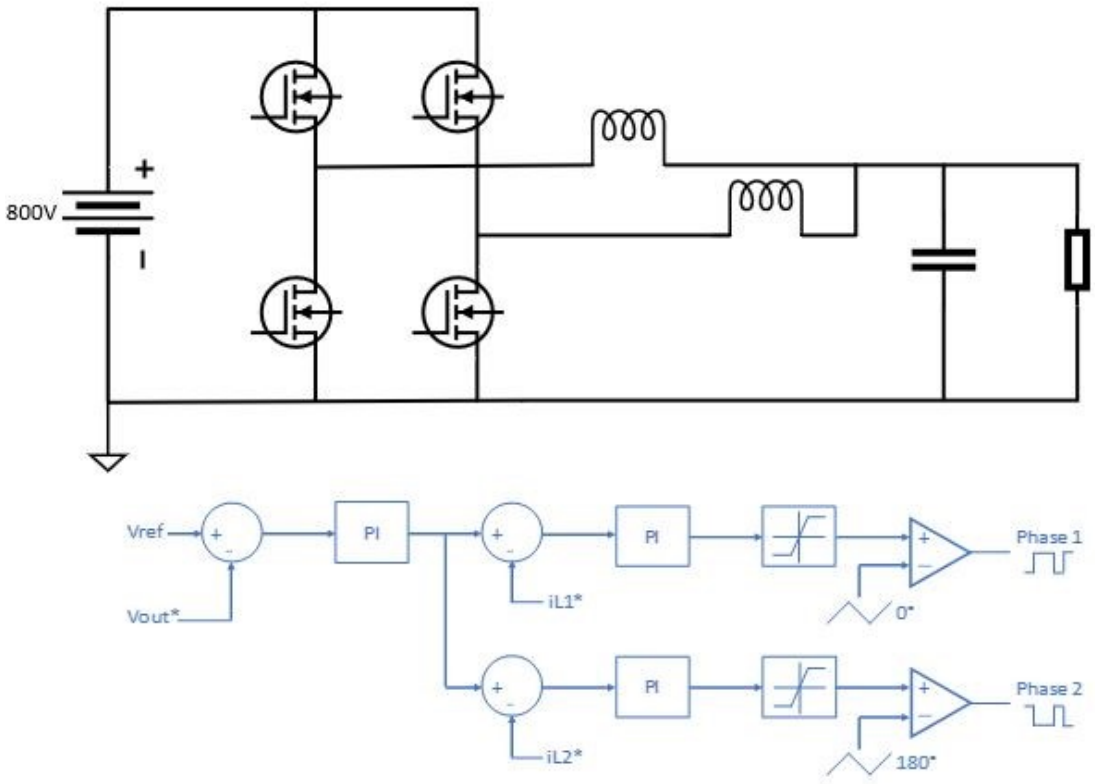

Figure 2.3: Bi-directional DC-DC converter operating as a buck, complete with PI controllers.

In addition, for the control logic, an outer voltage loop with voltage reference and PI controller was established. Then an inner current loop was inserted for each of the phase legs, each with a PI controller and comparator to generate the gate switching voltage.

2.2.2 Results

The front-end interleaved DC-DC converter worked as intended by bucking 800V from the battery source to 400V at the output while operating at a switching frequency of 20kHz. It was tested at heavy and light loads, as well as a nominal load without any issue.

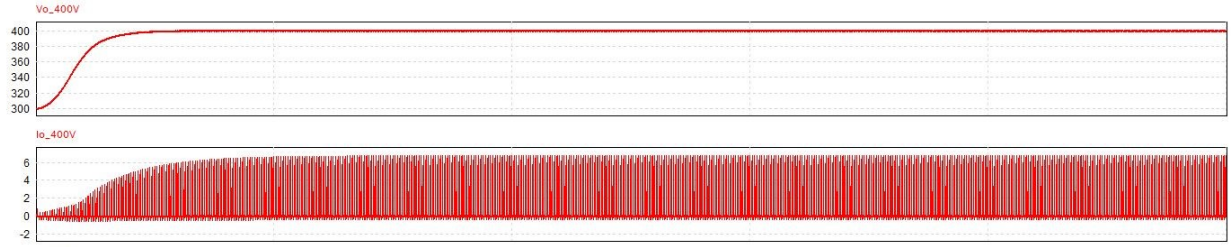

Figure 2.4: Interleaved DC-DC output voltage and current waveforms.

The output voltage ramped up to 400V with a modestly tuned PI controller in under 2 milliseconds. For this design, 400V was the designated reference for the output, however, it also compensated nicely when the output reference was changed from 350-450V. The output current of the buck looks as expected because it is cascaded with the full bridge converter. Charge in the primary coil flows in opposite directions due to the polarity being switched at each half cycle [9].

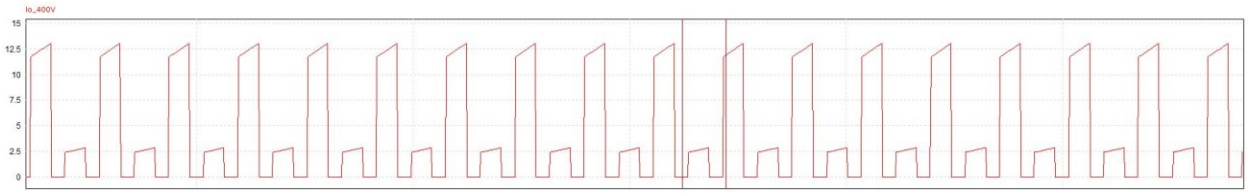

Figure 2.5: Interleaved DC-DC output current zoom waveform view.

There is also an adequate amount of dead time placed between switching cycles. Looking at the waveform, the current is reduced to zero momentarily. This is a common practice when designing converters of this topology to avoid turning on switches in the same leg; doing so would cause a short circuit of the high voltage bus potentially leading to a switch failure due to incredibly high di/dt current. Lastly, the DC-DC converter remained in CCM mode during heavy load as well as light load conditions. The inductor ripple current was monitored and remained around 2A peak to peak.

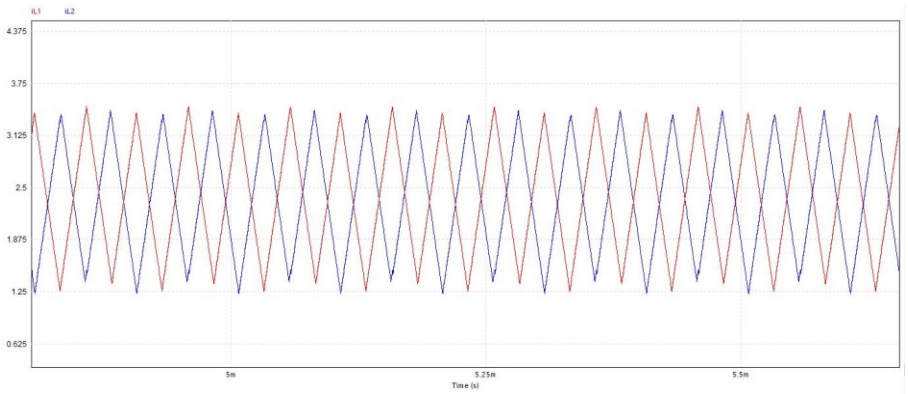

Figure 2.6: 2-Phase interleaved DC-DC inductor ripple current zoomed view.

2.3 Isolated Full Bridge Converter

2.3.1 Overview

The backend of the cascaded DC-DC topology was chosen to be an isolated center tap full bridge converter with a switching frequency of 50kHz. This configuration is common for applications above 1kW that require significant voltage conversion and isolation between the high voltage and low voltage sources. Industry standards like UL2202 require that all high voltage components in an EV must be isolated from the vehicle chassis, which acts as the 12V return [10]. Galvanic isolation is a preferred method for isolating such systems because magnetic fields can attain high power densities while remaining extremely efficient. The output voltage of the full bridge is equal to the input voltage, duty cycle, and most importantly, the primary to secondary winding turns ratio – this can be seen in Equation (7).

$$V_{OUT} = 2 \times V_{IN} \frac{N_2}{N_1} \times D \tag{7}$$

The circuit is comprised of four MOSFETs, a transformer, two diodes, and an output filter. An inductor and capacitor form the output filter and are sized based on the loads output voltage and current ripple requirements.

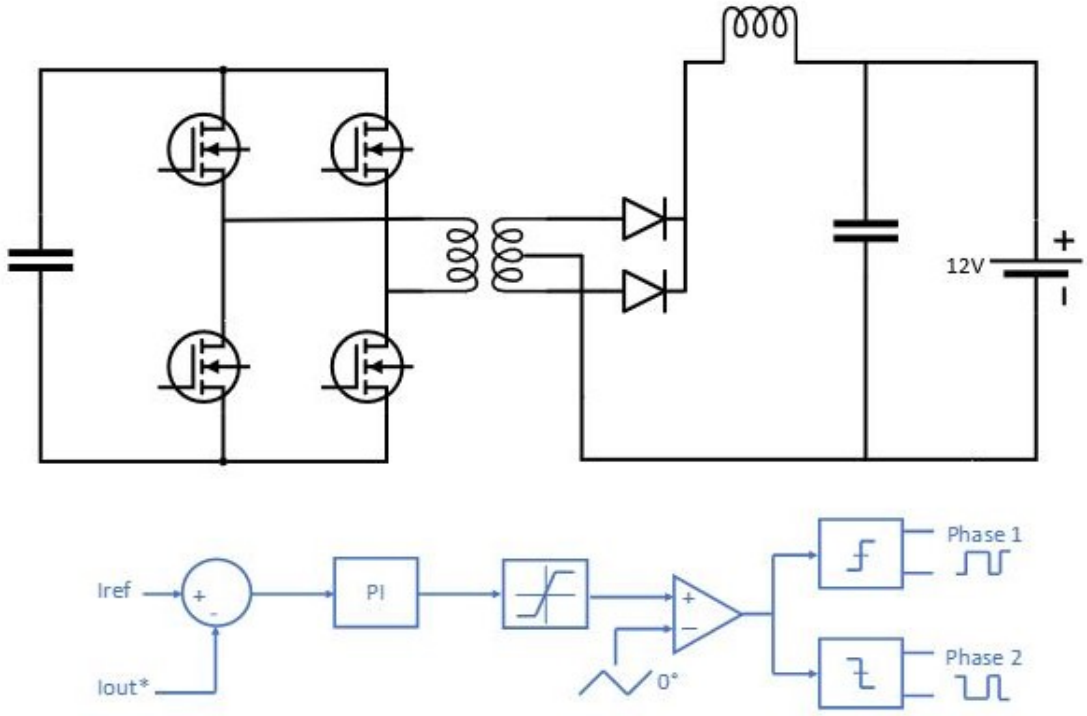

Figure 2.7: Isolated full bridge DC-DC converter with control scheme.

In modern EVs, converters of this nature are normally sized between 2-3kW so that was used for a design reference. The converter was tested at heavy and light loads of 200A and 50A respectively.

2.3.2 Results

The isolated full bridge DC-DC operated as designed by converting the 400V input from the interleaved buck to ~14V in order to power 12V loads as well as charge the 12V battery if

necessary. Constant voltage or constant current can both be achieved. The circuit reached steady-state in about 2 milliseconds across all operating conditions.

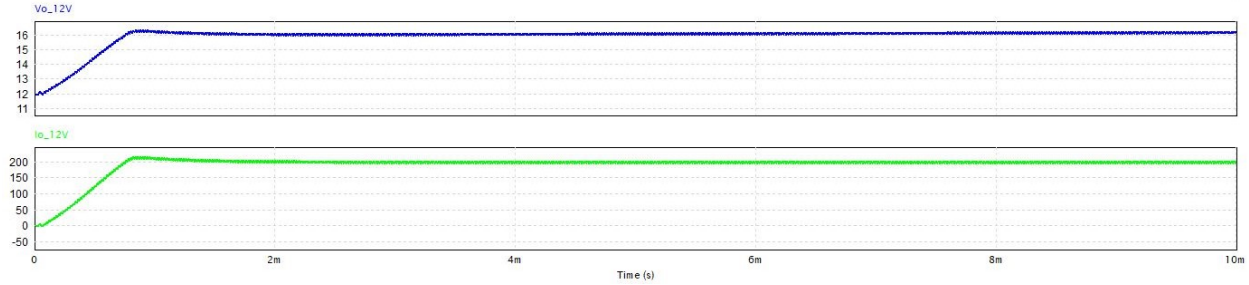

Figure 2.8: Isolated full bridge DC-DC output waveforms for heavy load.

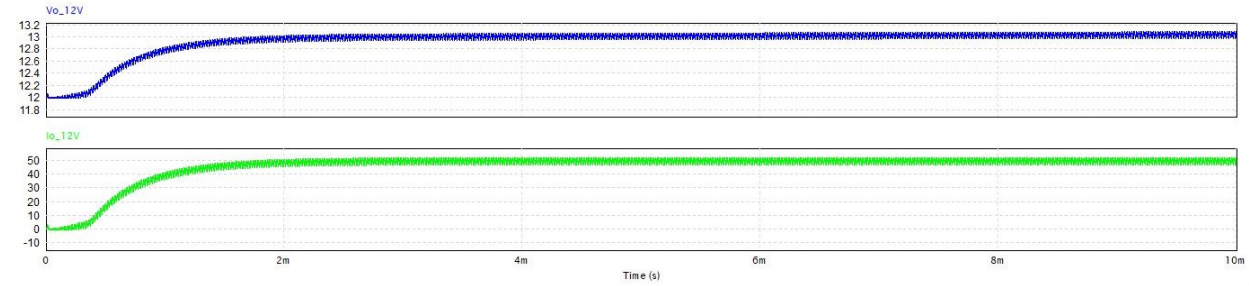

Figure 2.9: Isolated full bridge DC-DC output waveforms for light load.

As shown, the converter successfully produces an output current of 200A at roughly 15.8V. At a lighter load of 50A, the converter produces an output voltage of 13V. The output inductor and capacitor are sized adequately for all modes of operation. At the nominal operating load, 125A and 14.5V, the output current has ripple of approximately 4.7A while the output voltage ripple is just less than 100mV.

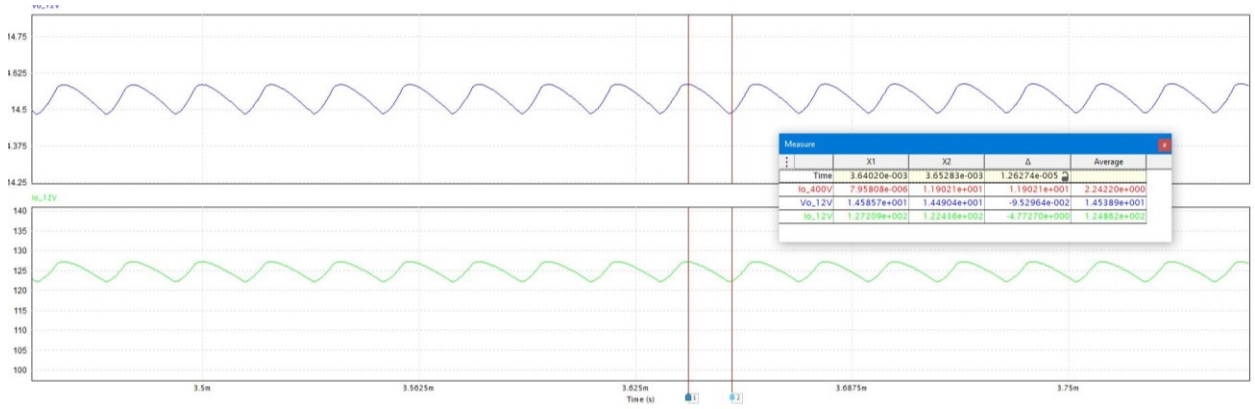

Figure 2.10: Isolated full bridge DC-DC output waveform ripple values.

Current and voltage ripple increased in the light load condition but CCM was maintained and the control loop was compensated appropriately.

Chapter 3: DC Fast Charging Operation

3.1 Introduction

As previously visited, DC fast chargers being deployed nationwide are capable of charging vehicles with bus voltages of 300-400V. EVs that begin to implement 800V architectures will be unable to utilize the infrastructure already in place. If properly designed, the interleaved converter can not only be used for propulsion, but as a way to boost the 400V source from modern DC fast chargers to levels required to charge an 800V bus. Using an existing converter onboard the EV for an additional use-case, as an intermediate solution, makes sense from a cost and mass perspective for vehicle manufacturers until 800V chargers are deployed. Other than DC fast charging, EVs will incorporate on-board chargers (OBCs) for 110V and 220V AC charging. These are necessary for customers who need a way to charge their vehicle at a residential or commercial property. The biggest downside to AC charging is the limitation in power, as a result, charging times are significantly longer. When off-board chargers are plugged into an EV, the OBC is bypassed to permit rapid, high power charging. 800V off-board charging stations with SiC technology are gaining popularity, but until they are deployed in massive quantities, the multipurpose bi-directional converter provides sufficient solution.

3.2 Charging the HV Bus

3.2.1 Overview

The high voltage bus can be charged with a traditional OBC or with a 400V DC fast charger by using the interleaved converter in reverse. In order to execute this multifunctionality, simple

HV connectors and contactors should be implemented at the node that joins the interleaved DC-DC and the full bridge converter. To perform in reverse, a secondary switch is required in place of the output diode. Diodes are passive components that only allow current to flow in one direction. This function is inherent to the diodes construction and will prevent a converter from operating in reverse.

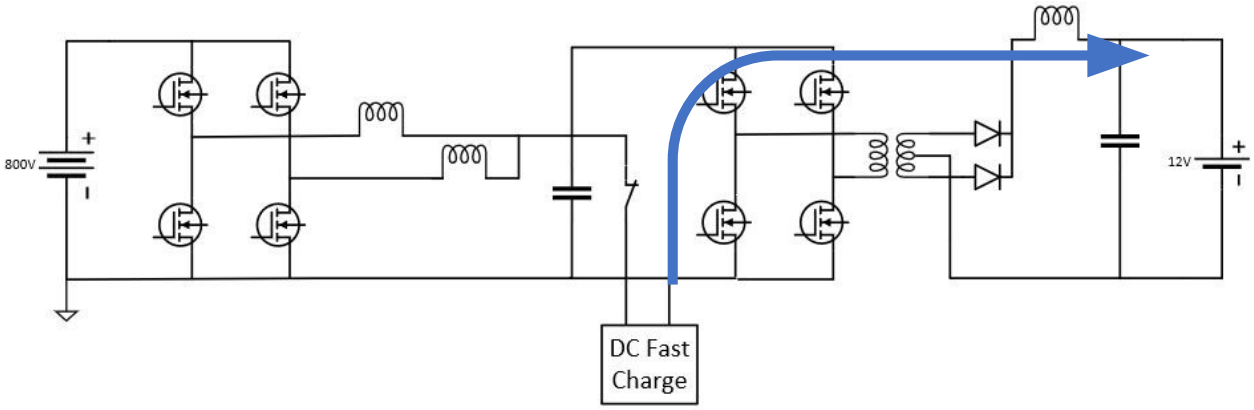

Figure 3.1: DC fast charging operation for the bi-directional DC-DC and full bridge converters.

The other necessity is that the inductor and capacitor for both converters are sized appropriately for both operation modes. A worst-case analysis should be completed to understand the power limitations of the components during the intended operating modes. The final element needed for the charging operation is a supplement control scheme. During low SOC conditions, phase 1 of charging will occur by using constant current. Revisiting Eq. (2) shows how the voltage is expected to rise linearly when a constant current is applied to a battery, which is essentially a very large capacitor. Once an appropriate SOC level is achieved, phase 2 of charging would begin by implementing constant voltage. During phase 2, the battery charge current decreases exponentially.

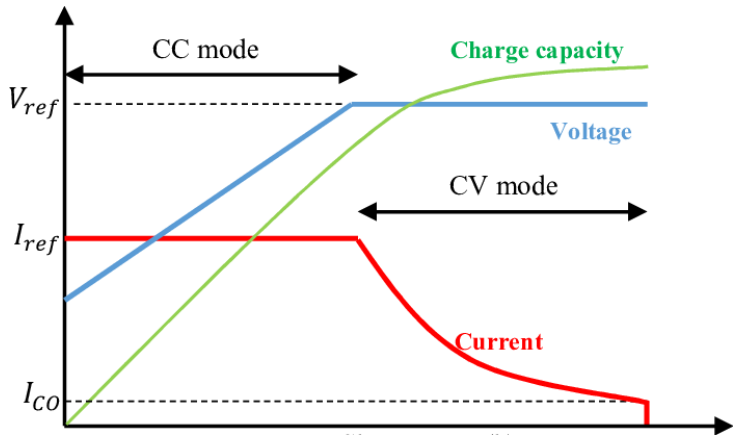

Figure 3.2: Charge profile of a lithium-ion battery.

During fast charging, if the 12V source also has a low SOC, the full bridge converter can be activated so that the 12V battery will also be charged. The same component sizing strategy and control logic will also apply to the full bridge DC-DC converter for the 12V system.

3.2.2 Results

The bi-directionality of the interleaved DC-DC converter worked as planned. An 800V battery model was constructed to replace the ideal voltage source that was originally used for simulating the motoring/forward operation. The original output of the interleaved DC-DC converter acts as the DC fast charging input, so a 400V ideal source was placed there accordingly. A separate control scheme was developed utilizing the same methodology as covered for the forward operation; an outer voltage loop with an inner current loop were applied along with PI controllers that required different tuning values. Upon review, a standard lithium-ion battery charging profile was implemented and tested. The battery is assumed to be at a low voltage and state-of-charge (SoC) that would indicate charging is required. During phase one the battery is charged with a constant current of 120A, as a result, the battery voltage increases linearly as expected.

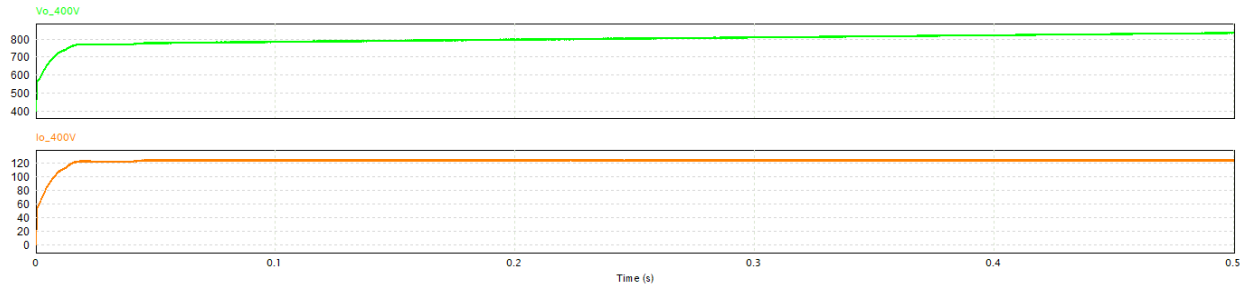

Figure 3.3: Charging the 800V battery with 100kW using constant current control.

The design of the charger was intended for 100kW by referencing contemporary DC fast charging systems. However, the converter can surely operate at higher power levels if needed. Phase 2 of charging entails applying a constant voltage to the battery. During this phase, charge current decreases exponentially. Rise in the lithium-ion battery SoC is quickest during the constant current charging phase.

3.3 12V Charging Results

The isolated full bridge converter can also utilize the DC fast charging mechanism as a means to charge the 12V source if necessary. The principles of charging a 12V lead acid or AGM are nearly identical as with the high voltage lithium-ion battery. Charging is staged with constant current being first, followed by constant voltage, and finished with a float charge.

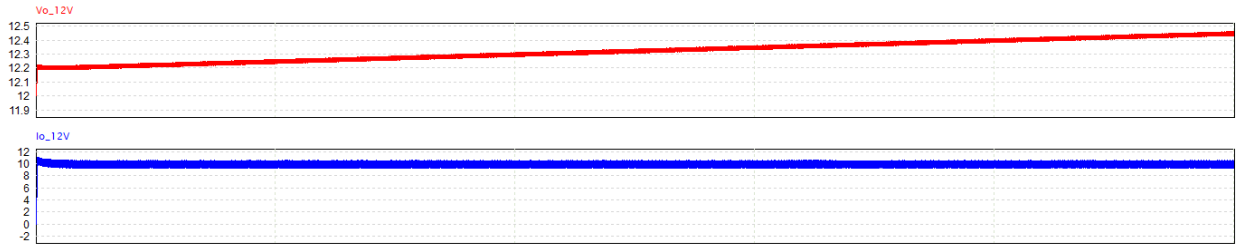

Figure 3.4: 12V charging utilizing the DC fast charging mechanism and constant current control.

Similar to the high voltage battery, the voltage of the 12V source rises linearly when constant current is applied. A separate control scheme was also developed and tuned for the full bridge to function correctly.

Chapter 4: Inverter Fault Detection and Compensation Strategy

4.1 Introduction

Advancements in the field of power electronics has significantly improved electric propulsion systems in almost every facet – power density, speed, and efficiency just to name a few. However, there is a growing concern over system reliability, specifically the reliability of semiconductor devices and electrolytic capacitors that prove to be the most vulnerable. The implication of this fact combined with a lack of redundancy indicates that any fault that should occur to the components or subsystems could potentially lead to the entire propulsion system becoming inoperable [11]. Further investigation reveals that power switching faults represent about 34% of all inverter faults [12]. This presents a worthy opportunity to develop and implement a solution to improve the reliability of the traction inverter. Not only would this benefit the manufacturer by reducing warranty costs, but it will also improve customer satisfaction. Likewise, there are also applications where continuous operation is extremely crucial and may even be required according to safety requirements. For these scenarios, a fault tolerant scheme should be implemented to improve system reliability. A fault tolerance solution should strive to feature a fast detection strategy, localization, and isolation of the component exhibiting the problem [11]. For this project, a single open switch fault detection strategy was developed and demonstrated. Faults of this nature can arise due to physical damage of the semiconductor device or because of problems with the gate driver circuit [13].

Single open-circuit faults become evident when monitoring the motor phase currents. For a voltage source inverter, typical for traction applications, single open-circuit faults are

characterized by the loss of the half-cycle current in the faulty phase. For example, if a fault occurs in the top-side switch, the current will be zero during the positive half-cycle. Likewise, if a fault occurs in the lower switch then the current will lose its negative half-cycle; the current will either be positive or zero [14], [15]. The following equation shows how the current changes between half-cycles in a fault induced phase.

$$i_b = \begin{cases} I_m \sin\left(\omega t - \frac{2\pi}{3}\right), & \frac{2\pi}{3\omega} < t \leq \frac{5\pi}{3\omega} \\ 0, & \frac{2\pi}{3\omega} < t \leq \frac{5\pi}{3\omega} \end{cases} \tag{8}$$

Additionally, because the PMSM is considered a balanced load, the current through the other two phases will increase in amplitude by a factor of √3. This presents an opportunity to detect this anomaly and react accordingly.

$$i_{sa}(t) = \frac{I_m}{2} \sin(\omega t) + I_{av} - \Delta i_a(t), Lower\ Fault \tag{9}$$

$$i_{sa}(t) = \frac{I_m}{2} \sin(\omega t) - I_{av} + \Delta i_a(t), Upper\ Fault \tag{10}$$

Several methods have been devised in order to detect and alleviate open switch faults based on inverter phase currents. Some of the more popular methods include: Park's vector, normalized DC current, spectrum analysis, wavelet-fuzzy, and wavelet-neural network [16].

4.2 Fault Detection Strategy

A reasonable expectation for a fault-tolerant propulsion system is the ability to operate with full performance after a fault occurs, or to at least operate in a degraded state that still meets the minimum requirements. It is also essential that vehicle safety is not hindered by the postfault operation due to noise or parasitic elements [17]. When choosing a fault detection scheme, certain factors should be considered to ensure a robust design. Several methods were researched based on the following design criteria [16].

I. Effectiveness: The method has the ability to successfully diagnose a faulty switch.
II. Immunity to Change in Load: The method should be robust against false positives that could occur during noisy conditions.
III. Detection Time: The method should detect and take appropriate action in a reasonable amount of time.
IV. Implementation Effort: The hardware, sensing algorithms, and mathematical operations should be relatively easy to incorporate into the circuit.

Upon the evaluation of several popular open-fault detection methods, a single strategy was identified for this project. The normalized DC current method, as it is commonly referred to, was chosen as the preferred fault-tolerant scheme. It is important to note that this method not only acts independent of the load, but it also proves to be the most reliable when compared against the other strategies [13], [16]. The normalized DC current method is based on monitoring and computing the average current values at each time step, normalizing the values, and comparing them to a predetermined threshold value. A current value greater than the threshold value would be

indicative of an open-circuit fault. Perhaps the greatest benefit in favor of this method, is the fact that the process is designed to work independent of the motor load. System parameters are unnecessary for implementation allowing for a straightforward calibration process [18]. It can be concluded that fault-tolerant drive systems that maintain full performance while remaining cost effective are increasingly desirable for automotive traction inverter applications [17].

4.3 Implementation

4.3.1 Overview

Interleaved DC-DC converters are perfect for implementing an inverter fault solution due to the fact that interleaved converters use multiple phases. As previously discussed, interleaving offers many benefits when compared with single-phase converters. When a second phase leg is added, current is shared between both phases 50-50, so the average DC current passing through the original inductor is cut in half. If for example, a phase becomes unavailable due to a trivial or non-catastrophic event, the converter will most likely still be able to operate, but at reduced power. Moreover, the converter is already connected in parallel with the inverter by using the same positive and negative references on the voltage bus. This presents an ample scenario to utilize a converter phase leg in the event that an inverter phase leg experiences a fault. A few contactors are all that is needed in order to swap the output of a DC-DC phase to operate as an inverting leg.

In order for the fault detection strategy to properly function, a few contactors had to be added to the schematic. In addition, the detection of the fault and control of the system were coded in C. Five contactors were placed in the circuit to properly control the flow of current and to rectify the degraded inverter phase. One contactor was placed at the output of the chosen converter phase such that it will open and cutoff the current path to the inductor once a fault is detected in the

inverter. A second contactor is similarly used in series with the motor phase. Contactor number three connects the appropriate motor phase current to the center point of the DC-DC half-bridge. The last two contactors are used to disconnect inverter phase C from the HV bus to prevent any complications to system performance due to electrical noise or unwanted parasitics.

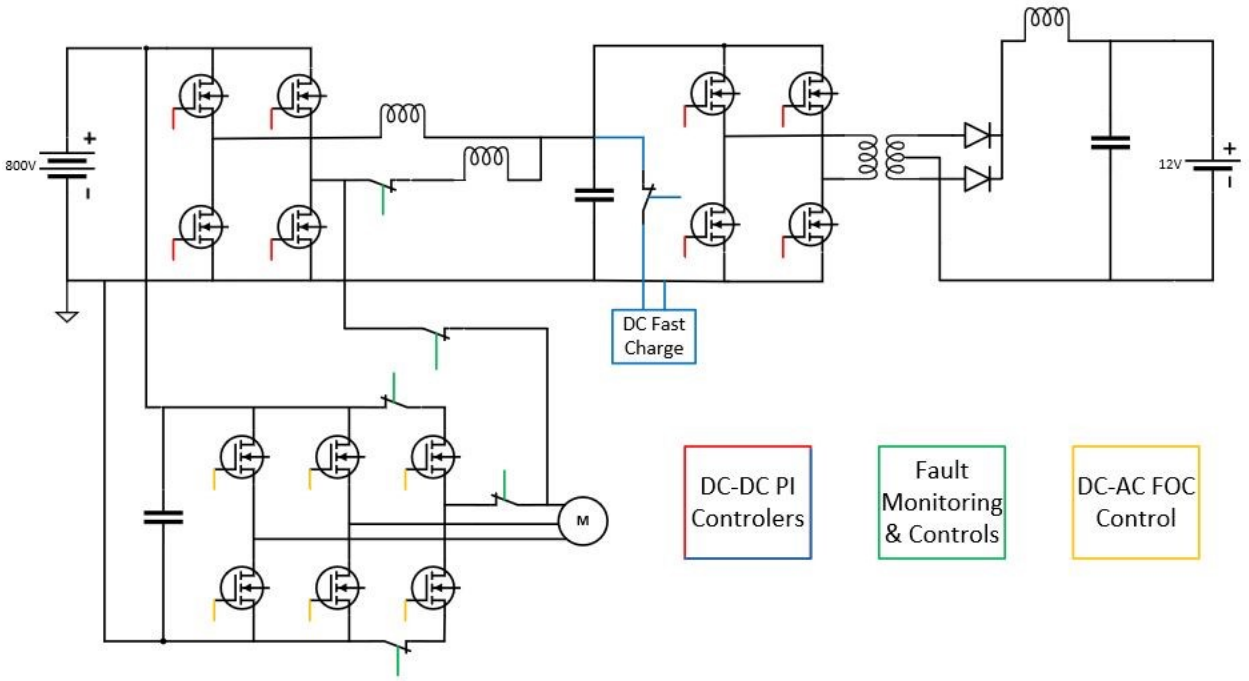

Figure 4.1: Implementation of the fault detection methodology for a single motor phase with a voltage source inverter and interleaved DC-DC converter.

The detection and rectification software were administered in C code. Phase currents are first measured with a sensor at the input of the motor. These AC values are converted into DC values by taking the RMS of each one.

Next, the values are normalized via the following operation in PSIM:

- X1 = Ia_RMS / (Ia_RMS + Ib_RMS + Ic_RMS)
- X2 = Ib_RMS / (Ia_RMS + Ib_RMS + Ic_RMS)
- X3 = Ic_RMS / (Ia_RMS + Ib_RMS + Ic_RMS)

The threshold value for detecting a fault was set at 0.15 for this application. A line of the detection code appears in PSIM as:

- (X1-X3) > 0.15 && (X2-X3) > 0.15

If the conditions are met, then an open switch fault has been detected. The signal is flagged and sent to the corresponding contactors as well as the switching controller for the DC-DC and inverter. Two other C blocks were also employed to seamlessly swap the DC-DC PWM control for FOC.

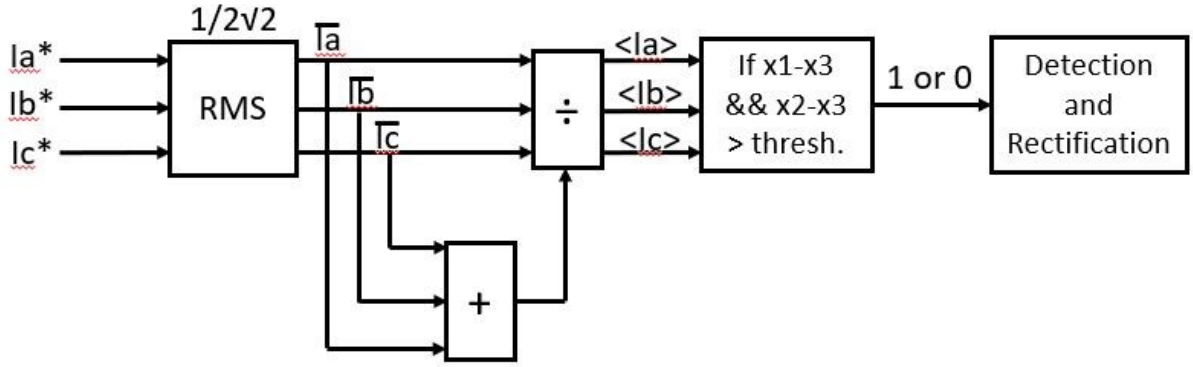

Figure 4.2: Inverter fault detection flow diagram using normalized DC current.

4.3.2 Results

The following section will review the results of imposing the inverter fault detection methodology by utilizing a single phase of the interleaved DC-DC converter. Figure 4.3 shows the normalized RMS currents of the motor over time. As can be seen, during steady-state the normalized current values should be ~1/3.

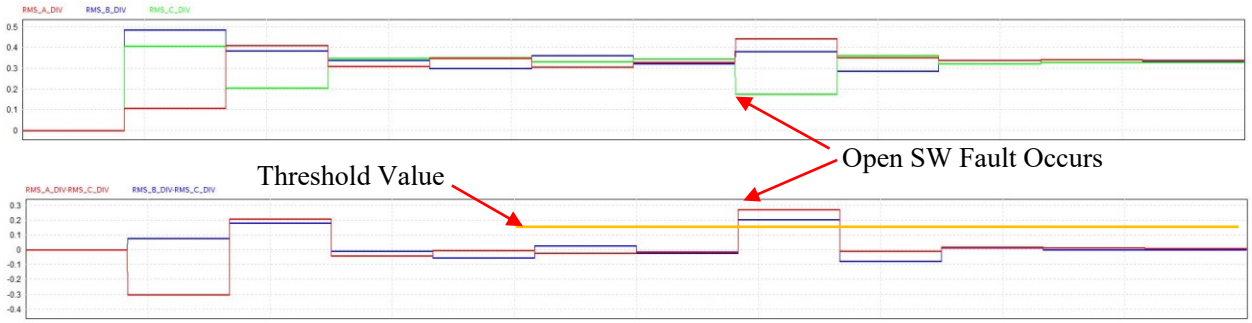

Figure 4.3: Normalized motor phase currents (top) and the difference in phase currents between phase C and phases A & B (bottom).

When an open switch fault occurs in a phase leg the current for half of the cycle will be equal to zero because the current is unable to flow through either the upper or lower switch. The outcome of this is that the current value of the faulty phase will decrease, and the amplitude of the functioning phases will increase by a factor of √3. This is to be expected because a PMSM is considered a balanced load [15]. In order to detect when a switch fault occurs, a threshold value should be chosen by calculating the expected increase in normalized current of the operational phases compared with the faulty phase.

The next figure captures the PWM signals for switches 3 and 4 in the interleaved DC-DC converter. During normal operation the switches are being commanded by the DC-DC control scheme to buck the 800V bus down to 400V for the full bridge converter. Once the switch fault is detected, the faulty inverter phase is rectified to prevent compromising system performance. Upon completion, a designated phase leg from the DC-DC is connected to the motor phase that experienced the switch fault. The DC-DC is already connected to the high voltage bus in parallel with the inverter so only the output of the phase needs to be rerouted. Once the hardware connections are in place, control of the switches are transitioned from a standard PWM strategy to FOC.

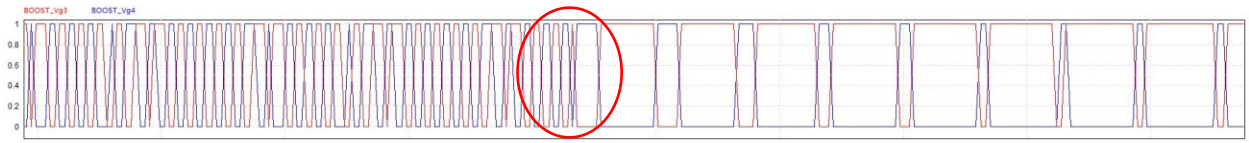

Figure 4.4: Transition of the interleaved buck converter phase leg from switching the DC-DC to switching the phase-C leg in the inverter during a switching fault.

Next we will begin to analyze the motor waveforms under a fault condition and its effect on the overall system. Figure 4.5 displays four different waveforms. Waveform (a.) is simply showing the switch in the inverter that experiences the fault. The switch is being controlled with the FOC scheme until a failure is induced which is why the gate signal goes to zero. The 3-phase motor currents are seen in waveform (b.). In this instant, the fault occurs at t = 0.1s in the upper-side switch of phase C. Current is unable to flow during the positive half cycle and becomes zero while current amplitude in phases A and B both increase by $\sim\sqrt{3}$. In about 20ms the fault is detected, the impaired inverter phase is rectified, and the selected DC-DC converter phase successfully drives phase C of the PMSM. In waveform (c.), the interleaved DC-DC loses a phase, but the output voltage only drops to about 395V and returns back to steady-state in less than 10ms. The last waveform, (d.), shows the two phases of the interleaved DC-DC and how phase two of the converter drops to 0A and phase one begins to supply the full load current.

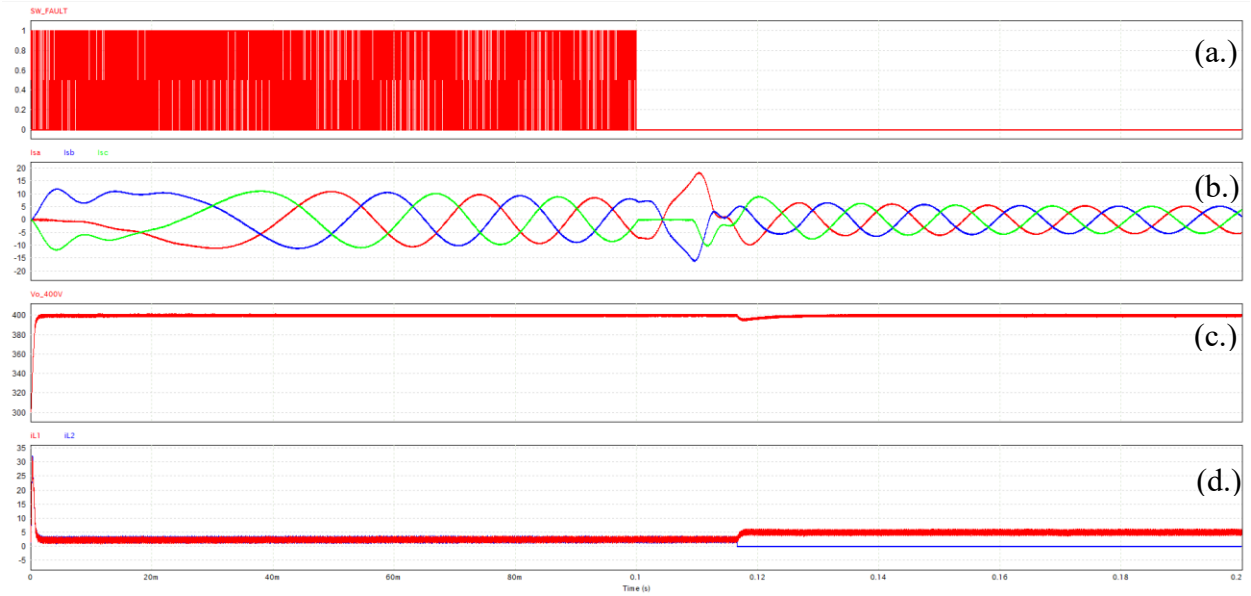

Figure 4.5: Mixed results for inverter SW fault, including a SW 5 switching fault (a.), 3-phase motor currents (b.), interleaved buck output voltage response (c.), and interleaved buck inductor phase currents (d.).

The intent of figure 4.6 is to show that the fault detection methodology is robust against false positives that may be caused by a change in load. Prior to 0.5s, the motor currents are in steady-state. At 0.5s, an increase in torque is commanded and the amplitude of the phase currents increases by about 2x. Steady-state of the motor current is once again realized until 1s where the speed is increased from 170rad/s to approximately 215rad/s. A false-positive is not seen in either case. An open switch fault is induced at 1.5s where it is detected and resolved in about 20ms. The waveform below the motor currents show the speed of the motor in comparison to the speed reference.

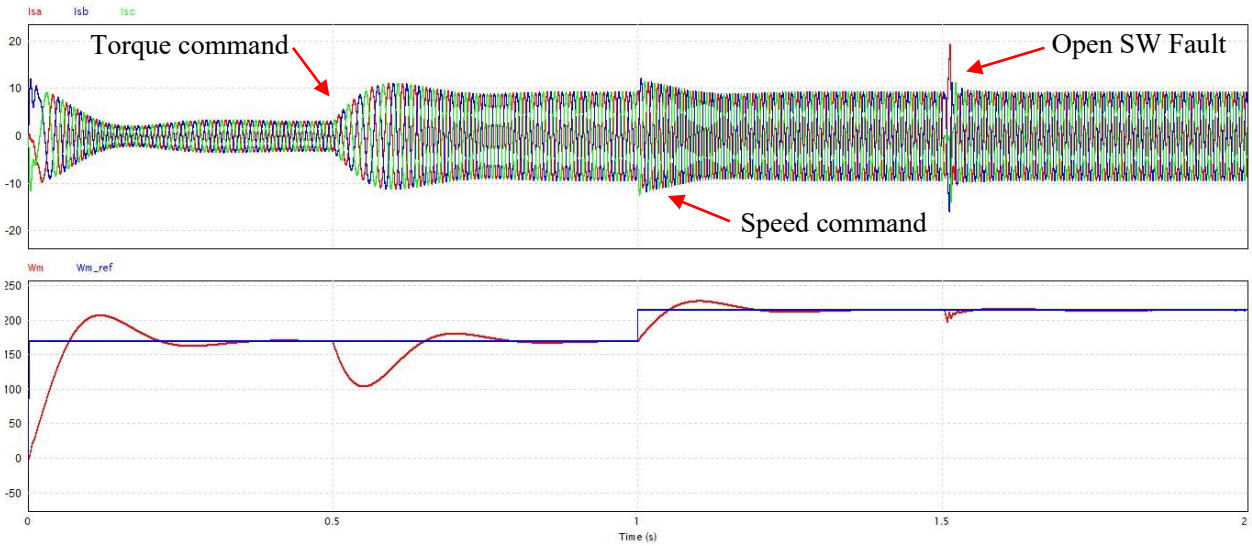

Figure 4.6: 3-phase motor current waveform during torque and speed reference changes as well as a switch fault (top) and in addition, the speed reference superimposed with the actual speed (bottom).

An intuitive fault detection strategy is implemented by normalizing the RMS current of the motor and comparing it to a calibrated threshold value. Hardware integration also remains relatively simple, only four switches are needed to completely rectify the damaged inverter phase and replace it with a phase from the DC-DC. This strategy ensures that full functionality of the propulsion system is maintained during a fault at expense to a degraded state of 12V accessories.

Chapter 5: Conclusion

Until recently, discrete IGBT devices and large multi-chip power modules have been the most widely used components in electric vehicle propulsion systems – including DC-AC traction inverters. Even so, wide-bandgap devices like SiC have properties that prove increasingly advantageous for the use in automobile electrification applications [19]. Moreover, there is a growing demand in the industry to reduce mass, lower complexity, and increase reliability of the electrical architecture.

The intent of this research was to analyze market trends and to come up with a solution to address emerging industry trends. Two practical converter topologies were cascaded together to form a solution flexible enough to serve multiple purposes in 800V architectures. During normal propulsion, the proposed DC-DC outputs a 12V source for accessories. The front-end of the cascaded converter features a bi-directional interleaved DC-DC that can boost the supply of a 400V DC fast charger to 800V for charging the high voltage bus of a SiC enabled powertrain. This serves as a cost-effective intermediate solution until SiC DC fast chargers are developed and deployed nationwide. Lastly, concerns have grown over the reliability of power electronic solutions, specifically semiconductor devices. If a power fault is induced into the electric propulsion system, the vehicle may become limited in function or cease to run at all. For this reason, an intelligible fault detection method was implemented by monitoring phase currents in the 3-phase AC motor. An algorithm was then designed to detect anomalies caused by an inverter open switch fault. Once a fault is detected, the damaged inverter phase is rectified and replaced by

a phase in the interleaved DC-DC structure. This strategy ensures that full functionality of the propulsion system is maintained during a fault at expense to a degraded state of 12V accessories. The PSIM simulation results verified the proposed power conversion structure and motor drive fault compensation scheme.

Appendix

PSIM schematic used for proposed electric powertrain.

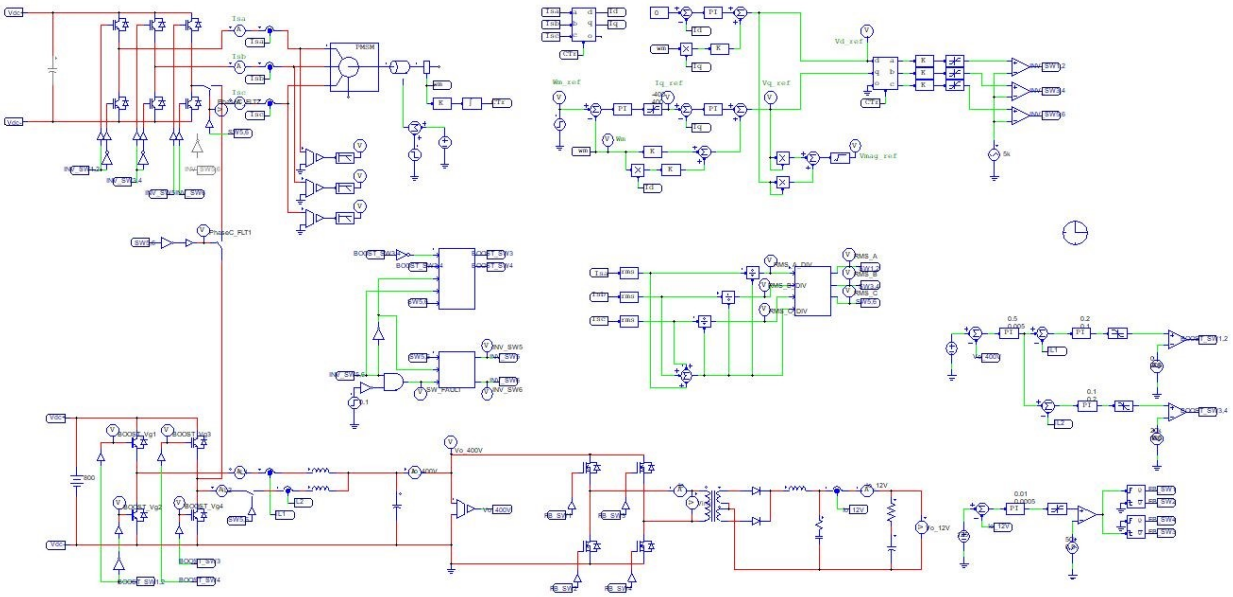

PSIM C code for function blocks.

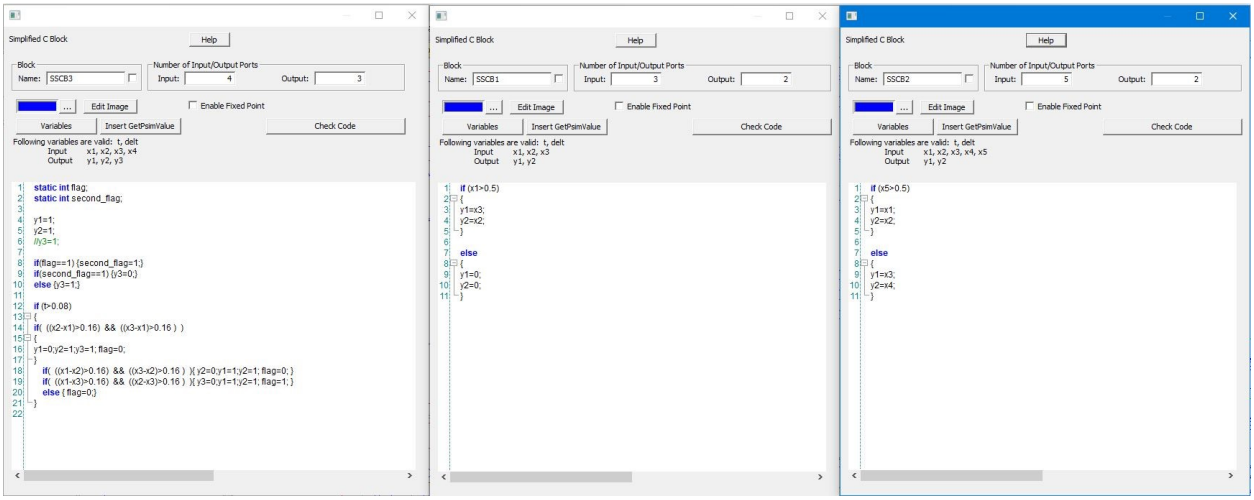

References

1. Texas Instruments Europe, “Field Orientated Control of 3-Phase AC-Motors,”1998. Available: https://www.ti.com/lit/an/bpra073/bpra073.pdf

2. S. L. Mantia, V. Giuffrida, S. Buonomo, “Benefits and advantages of using SiC,” STMicroelectronics Munich Germany, PCIM Europe, 978-3-8007-4938-6, 2019.

3. E. Wiesner, K. Masuda, M. Joko, “New 1200V full SiC module with 800A rated current,” 2015 17th European Conference on Power Electronics and Applications, 2015.

4. K. Doyle, “Level Up Your EV Charging Knowledge,” ChargePoint, 23-Mar-2017. [Online]. Available: https://www.chargepoint.com/blog/level-your-ev-charging-knowledge/. [Accessed: 01-Aug-2020].

5. “Fast-Charging the EV Market,” Wolfspeed Power & RF, 25-Feb-2020. [Online]. Available: https://www.wolfspeed.com/knowledge-center/article/fast-charging-the-ev-market. [Accessed: 01-Aug-2020].

6. “Vitesco Technologies and ROHM cooperate on silicon carbide power solutions,” ROHM, 04-Jun-2020. [Online]. Available: https://www.rohm.com/news-detail?news-title=vitesco-and-rohm-cooperate-on-sic-power-solutions&defaultGroupId=false. [Accessed: 01-Aug-2020].

7. M. O’Loughlin, “An Interleaving PFC Pre-Regulator for High-Power Converters,” Texas Instruments. Available: https://www.ti.com/lit/wp/slua746/slua746.pdf?ts=1595220117968&ref_url=https%253A%252F%252Fwww.google.com%252F

8. T. Eichorn, “Estimate Inductor Losses Easily in Power Supply Designs,” Maxim Integrated Products, 01-Apr-2005. [Online]. Available: https://www.powerelectronics.com/content/article/21861355/estimate-inductor-losses-easily-in-power-supply-designs

9. A. Singh and J. VS, “Voltage Fed Full Bridge DC-DC and DC-AC Converter for High-Frequency Inverter Using C2000,” Texas Instruments, Jan. 2018.

10. C. Yao, “Semiconductor Galvanic Isolation Based Onboard Vehicle Battery Chargers,” Ohio State University Dissertation , 2018.

11. Y. Song and B. Wang, “Survey on Reliability of Power Electronic Systems,” IEEE Transactions on Power Electronics, vol. 28, no. 1, Jan. 2013.

12. D. U. Campos-Delgado, E. Palacios, and D. R. Espinoza-Trejo, “Fault-tolerant control in variable speed drives: A survey,” IET Elect. Power Appl., vol. 2, no. 2, pp. 121–134, Mar. 2008.

13. W. Sleszynski, J. Nieznanski, and A. Cichowski, "Open-Transistor Fault Diagnostics in Voltage-Source Inverters by Analyzing the Load Currents," IEEE Transactions on Industrial Electronics, vol. 56, no. 11, pp. 4681-4688, 2009.

14. Z. Jian-Jian, C. Yong, C. Zhang-Yong, and Z. Anjian, “Open-Switch Fault Diagnosis Method in Voltage-Source Inverters Based on Phase Currents,” IEEE Access, vol. 7, pp. 63619–63625, 2019.

15. S. K. E. Khil, I. Jlassi, J. O. Estima, N. Mrabet-Bellaaj, and A. J. M. Cardoso, “Detection and isolation of open-switch and current sensor faults in PMSM drives, through stator current analysis,” 2017 IEEE 11th International Symposium on Diagnostics for Electrical Machines, Power Electronics and Drives (SDEMPED), 2017.

16. B. Lu and S. Sharma, “A Literature Review of IGBT Fault Diagnostic and Protection Methods for Power Inverters,” 2008 IEEE Industry Applications Society Annual Meeting, 2008.

17. M. Naidu, S. Gopalakrishnan, and T. Nehl, “Fault-Tolerant Permanent Magnet Motor Drive Topologies for Automotive X-By-Wire Systems,” IEEE Transactions on Industry Applications, vol. 46, no. 2, pp. 841–848, 2010.

18. V. H. V. Fnu, “Fault Tolerant Power Conversion System with Interleaved Hybridized Energy Storage Systems for a PMSM Traction Motor Drive in Electrified Powertain,” University of Michigan - Dearborn Thesis, 2020.

19. S. L. Mantia, V. Giuffrida, S. Buonomo, “Benefits and advantages of using SiC,” PCIM Europe 2019; International Exhibition and Conference for Power Electronics, Intelligent Motion, Renewable Energy and Energy Management, 2019.

20. B. D. E. Cherif, A. Bendiabdellah, MokhtarBendjebbar, and L. Souad, “A Comparative Study on Some Fault Diagnosis Techniques in Three-Phase Inverter Fed Induction Motors,” IntechOpen, 05-Nov-2018. [Online]. Available: https://www.intechopen.com/books/fault-detection-and-diagnosis/a-comparative-study-on-some-fault-diagnosis-techniques-in-three-phase-inverter-fed-induction-motors. [Accessed: 31-Jul-2020].

21. S. A. Gorji, H. G. Sahebi, M. Ektesabi, and A. B. Rad, “Topologies and Control Schemes of Bidirectional DC–DC Power Converters: An Overview,” IEEE Access, vol. 7, pp. 117997–118019, 2019.

22. S. Haghbin, “Design considerations of a 50 kW compact fast charger stations using nanocrystalline magnetic materials and SiC modules,” 2016 Eleventh International Conference on Ecological Vehicles and Renewable Energies (EVER), 2016.